Using Immunology Principles for Fault Detection

P. J. Costa Branco, *Member, IEEE*, J. A. Dente, and R. Vilela Mendes

***Abstract*—The immune system is a cognitive system of complexity comparable to the brain and its computational algorithms suggest new solutions to engineering problems or new ways of looking at these problems. Using immunological principles, a two- (or three-) module algorithm is developed which is capable of launching a specific response to an anomalous situation for diagnostic purposes. Experimental results concerning fault detection in an induction motor are presented as an example illustrating how the immune-based system operates, discussing its capabilities, drawbacks, and future developments.**

***Index Terms*—Fault diagnosis, immune-based systems, induction motors, learning systems.**

I. Introduction

THE immune system, with its cell diversity and variety of information processing mechanisms, is a cognitive system of complexity comparable to the brain. Understanding the way this organ solves its computational tasks suggests new engineering solutions or new ways to look at old problems.

Early fault detection and predictive maintenance are extremely important for the cost savings they provide, especially in large and complex systems with many pieces of equipment such as, for example, an electrical power network. In a system of such complexity (because of its many connections and diversity of equipment) it is difficult to make a complete catalog of all the possible, and probable, anomalous situations. On the other hand when, for example, a circuit breaker operates in response to an overload, the harm is already done, either to some equipment or to the stability of the network. With its ability to detect and react to novel situations and to unleash smooth early secondary responses, the immune system seems to be an adequate source of inspiration to develop algorithms for early detection of anomalous behavior in electrical systems.

After a short introduction to the characteristics of the immune system that are relevant for our purposes, this paper describes a three-module algorithm for anomaly detection. By analogy with the immune system, these modules will be called the B-module, the T-module, and the D-module. However, it should be emphasized that we are not trying to imitate the immune system in all its features and detailed operation. The proposed algorithm is inspired in the current understanding of the mammal immune system although, in detail, it does not exactly follow the biological steps. Many of the detailed features of the immune system are dependent on the biological context where it operates and on the type of cell hardware that is used. It is our opinion that the correct way to profit from the clever evolutionary mechanisms developed by nature is to obtain algorithmic inspiration from them, but, at the same time, to find the implementation that is more appropriate for our problem. For example, the interaction between the B-module and the T-module takes the reverse order of what is found in nature, with a clone proliferation phase preceding T-identification. Clone proliferation is a costly biological operation, whereas, in the software for an anomaly detection system, it is merely a virtual (not very time consuming) operation. Therefore, it makes sense to reverse the operations to improve identification accuracy. This is a good example of why one should receive inspiration from nature but not copy it blindly.

The algorithmic modules developed in Section II have a wide range of applications to many different technological systems. As an illustration of how the proposed immune-based algorithm operates, a concrete case is dealt with in the last part of the paper, namely, an application to anomaly detection in induction motors. Experimental results are presented, discussing the algorithm capabilities, drawbacks, and its future developments.

Manuscript received June 25, 2001; revised April 9, 2002. Abstract published on the Internet February 4, 2003.

P. J. Costa Branco and J. A. Dente are with the Laboratório de Mecatrónica, DEEC, Instituto Superior Técnico, 1096 Lisbon Codex, Portugal (e-mail: pbranco@alfa.ist.utl.pt; edentepc@alfa.ist.utl.pt).

R. Vilela Mendes was with the Laboratório de Mecatrónica, DEEC, Instituto Superior Técnico, 1096 Lisbon Codex, Portugal, and also with the Zentrum für interdisziplinäre Forschung, Universität Bielefeld, 33615 Bielefeld, Germany. He is now with the Laboratório de Mecatrónica, DEEC, Instituto Superior Técnico, 1096 Lisbon Codex, Portugal (e-mail: vilela@cii.fc.ul.pt).

Digital Object Identifier 10.1109/TIE.2003.809418

II. Immune System Paradigm

Some of the immune system features that are of interest for anomaly detection in complex technological systems are as follows [1]–[7].

- *Uniqueness*: The immune system of each individual is unique, each one being a different entity, in spite of their overall similarity. Similar pieces of equipment are also unique entities. For instance, electric motors of the same type and with equal ratings have different aging processes when placed in different electrical and thermal stress conditions. Therefore, they also require a protection system that is tuned to their specific vulnerabilities.
- *Imperfect detection and mutation*: By not requiring an absolutely precise identification of every pathogen, the immune system becomes flexible and increases its detection range. However, when a pathogen is detected, a hypermutation mechanism sharpens the identification. Because identification of pathogens is made by partial matching, a small number of the "detectors" (10^8 to 10^{12}) is able to recognize nonself patterns on the order of 10^{16}. Similarly, it is not an easy task to characterize precisely all the possible anomaly situations in a complex system. Therefore, an initial rough characterization of the anomalies and imperfect detection seems an useful feature. That is, initially

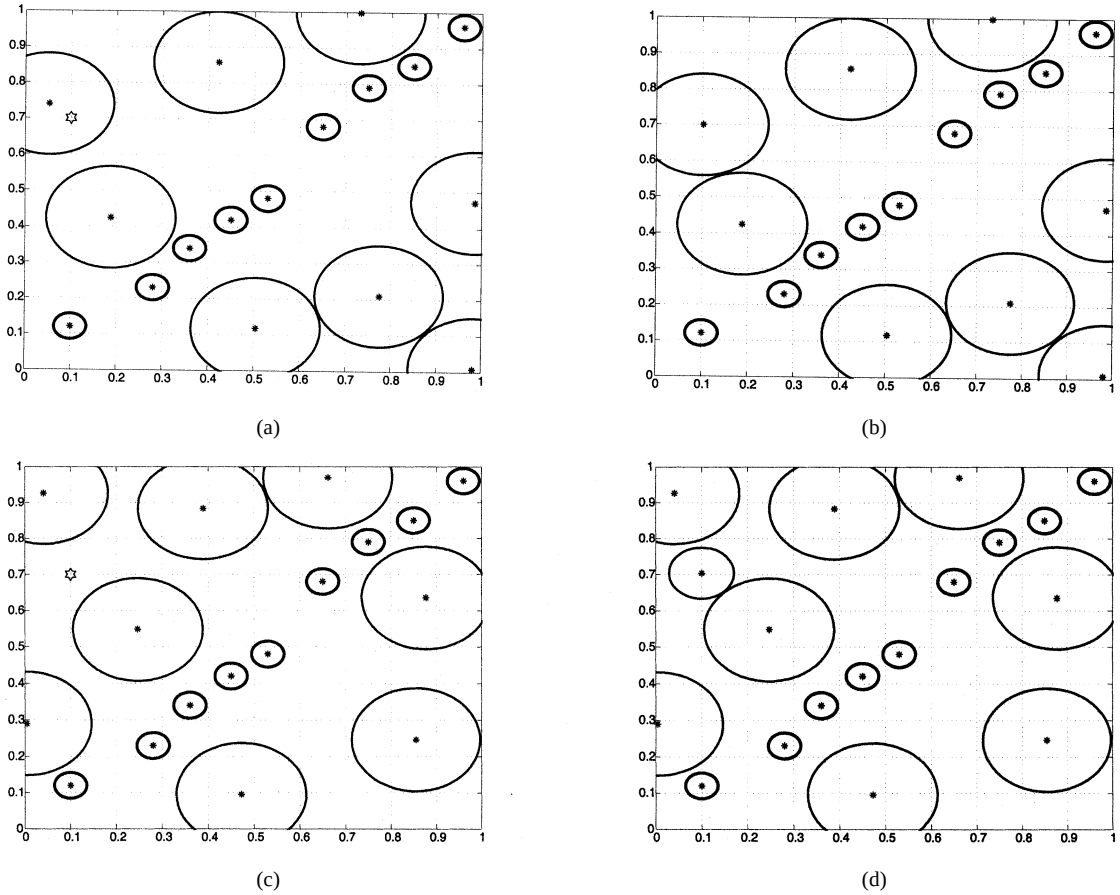

Fig. 1. T-module structure. (a) Self patterns (small circles) and anomaly detectors (large circles). (b) Shift of a detector code to increase affinity with an anomaly. (c) An anomaly outside all detector neighborhoods. (d) Creation of a new detector.

a small number of detectors may be defined, which are at a later stage modified by the dynamics.

- *Learning and memory*: The immune system is able to learn the structure of the pathogens, and remember those structures. Future responses are much faster and, when made at an early stage of the infection, no adverse effects are felt by the organism. We underline the importance of this feature for smooth operation and cost savings, both in fault detection and in preventive maintenance.
- *Novelty detection*: The immune system can detect and react to pathogens that the body has never encountered before.
- *Distributed detection*: The detectors used by the immune system are small and efficient, highly distributed and not subjected to centralized control.

III. Algorithm

In the algorithm, the states of the system, both *normal condition* and *anomaly* states, are characterized by the values of N variables. The N-dimensional state vector is normalized in such a way that all variables take values in the interval $[0, 1]$. The values of the state vector in normal conditions define the *self* S of the system. The anomaly states are the *nonself* of the system.

The algorithm contains three modules. The T-module discriminates self from nonself (that is, from anomalies). The B-module reacts to all frequently occurring state vector values (self and nonself codes) and presents its results to the T-module. The B-module also plays a role in updating the T-module. For large distributed systems one considers also the implementation of D-modules which are essentially reduced state space T-modules. They are simple anomaly detection units that, when some potential abnormal situation is detected, report the situation to a central system which then makes a detailed analysis of the event.

A. T-Module

This module contains a set of detectors which are vectors in complementary space of the self, $A = [0, 1]^N \backslash S$. Each element $\vec{x}$ of A is able to detect anomalies inside a radius r_x around it. That is, if $\mid \vec{y} - \vec{x} \mid < r_x$, $\vec{y}$ being the current state of the system, an anomaly of type x is reported.

Let the set of self patterns be known. Then, the algorithm defines d detectors with radius r_x. Fig. 1(a) illustrates, in a two-dimensional space, the basic idea. The small circles are the self patterns. To each point in the self corresponds a code (a set of vector coordinates) and an affinity neighborhood of normal operating conditions inside a radius r_s. The anomaly detectors are shown in the figure as large circles. The T-module is initialized by choosing points in A at random with corresponding radius r_x, until a reasonable coverage of the space A is obtained with d detectors.

The T-module receives inspiration from the censoring mechanism for T-cells that occurs in the thymus. This negative selection process is implemented in the T-module as follows. Each candidate anomaly detector (immature T-detector) is generated at random. The affinity of this vector with those defining the self and the other already established detectors is measured by the Euclidean distance. If the new detector falls in the neighborhood domain of another detector or of a self code, it is deleted and another candidate detector is generated at random. Otherwise, the detector is included as an element $\vec{x}$ of the space A (mature T-detector). The censoring mechanism is repeated until a prespecified number d of detectors is generated.

When a measurement $\vec{y}$ of the system arrives at the T-module, the algorithm verifies whether this code has affinity with one of the detectors or with the self. If it falls in the self domain, no detector is activated. If affinity is found with one of the detectors $\left(\vec{x'}\right)$, an anomaly of type $\vec{x'}$ is reported. To avoid overreaction to spurious situations, each detector is equipped with a counter and reports an anomaly only if the offending vector occurs more than a predefined number of times.

We notice at this point that, with random initialization, the T-module is not necessarily tuned to the most frequent, or probable, anomalous situations. On the other hand, some dangerous gaps may occur between the neighborhood domains of the detectors. This situation is corrected by dynamic interaction with the B-module.

By a mechanism to be described later on, the B-module generates vector codes corresponding to the most frequently occurring states of the system and sends these codes as *alert codes* to the T-module. When an alert code $\vec{\hat{x}}$ coming from the B-module arrives to the T-module, the latter takes one of three actions.

1) If $\vec{\hat{x}}$ is located inside a detector, the center of this detector is shifted to a position closer to the $\vec{\hat{x}}$ code and, if $\vec{\hat{x}}$ continues to occur, an anomaly is reported. That is, not only is an anomaly detected but also the detector becomes better tuned to this kind of anomaly.
2) If $\vec{\hat{x}}$ is located outside all detector neighborhoods, at a distance at least r', a new detector is created at the position of the $\vec{\hat{x}}$ code with radius r'. As before, if this situation recurs, an anomaly is reported.
3) Finally, if $\vec{\hat{x}}$ has affinity with a self pattern, nothing happens.

By itself or in interaction with the B-module, the T-module is an adaptive system. As an illustration, two typical situations are considered here. The first one is shown in Fig. 1(a) and (b). Suppose that a nonself code [the star symbol in Fig. 1(a)] is detected several times. Then, the detector changes its code to increase the affinity to this type of anomaly, as shown in Fig. 1(b). The second situation, shown in Fig. 1(c), corresponds to a case in which no detector had affinity with the external code. In this case, if the situation occurs many times, the algorithm creates a new detector with a resolution defined by the smallest distance to the other detector boundaries, as shown in Fig. 1(d). In this way, the T-module modifies the initial set of detectors produced by the censoring mechanism. It may change their number, modify the space distribution and change the resolution, creating a system-specific anomaly detection device.

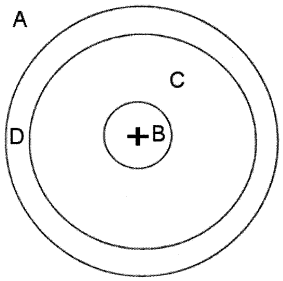

Fig. 2. Zones A–D for the mutation process.

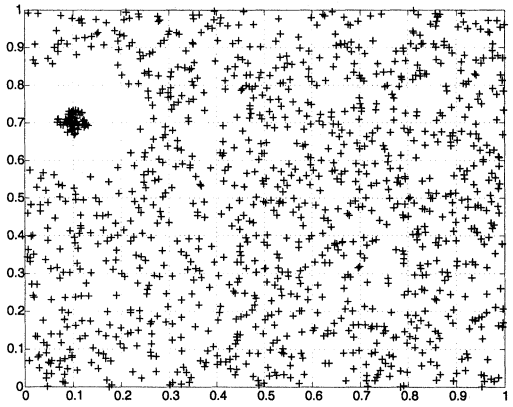

Fig. 3. Mutation creates a cluster around an external code.

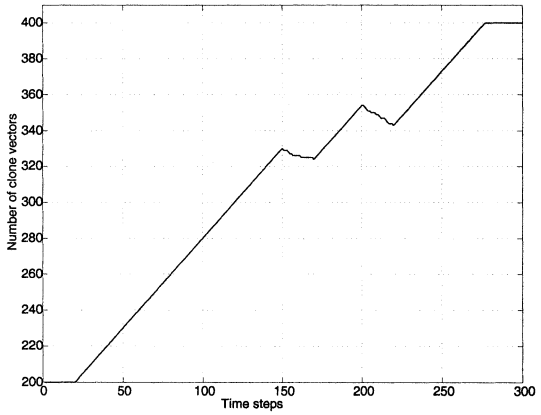

Fig. 4. Evolution of the clone population.

B. B-Module

The B-module plays a role in improving the A space coverage of the T-module and, when used with a system that is known to be operating in normal conditions, may also be used to generate the self patterns.

Fig. 5(b) shows an example of a typical B-module. It has a total population of N_t vectors

$$N_t = N_l + N_{l_c} \tag{1}$$

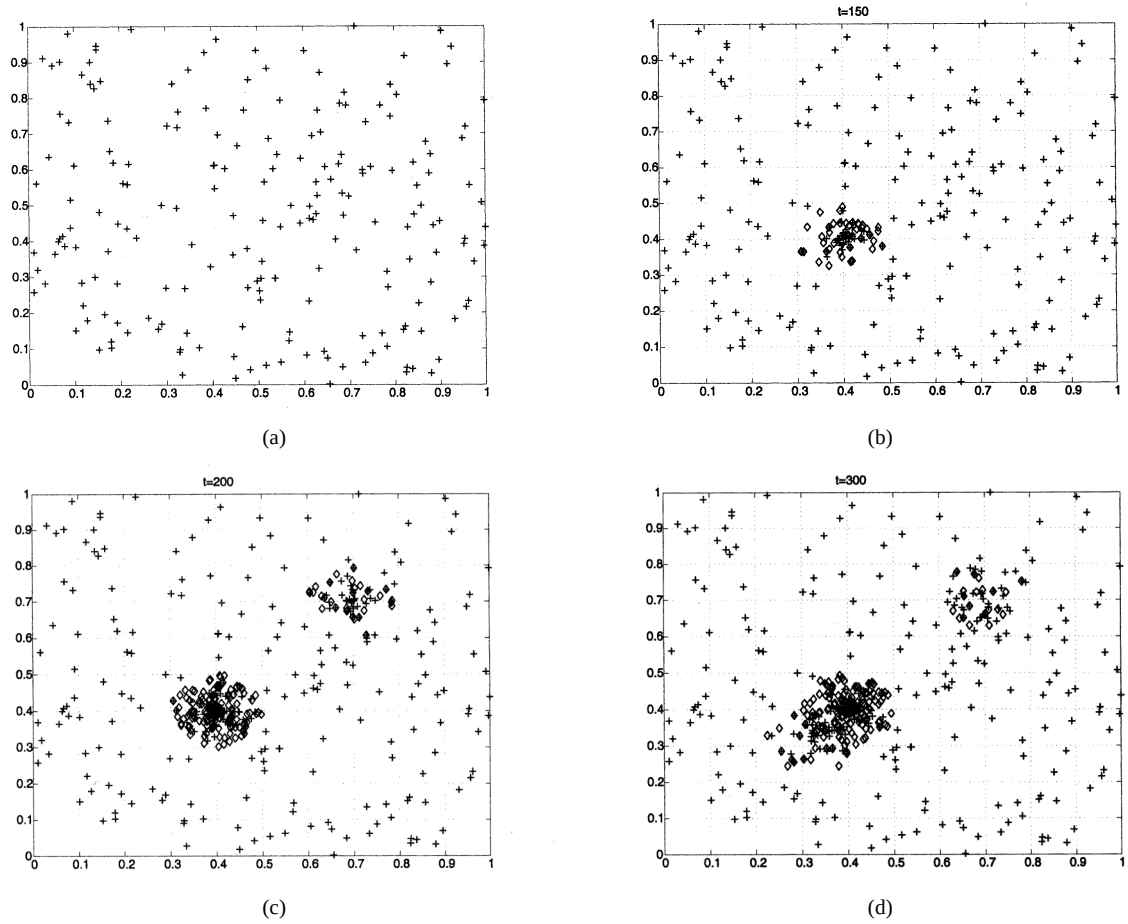

Fig. 5. (a) Initial vector population. (b) Population (initial + plus clones ⋄) at $t = 150$, (c) $t = 200$ and (d) $t = 300$.

consisting of an initial population of N_l vectors $\left\{\vec{x_l}\right\}$, the "+" symbols randomly distributed in the whole space $[0,1]^N$, plus a variable number N_{l_c} of clone vectors $\left\{\vec{x_{l_c}}\right\}$, the "⋄" symbols also shown in Fig. 5(b).

The number of clone vectors changes as the system evolves. To keep the system computationally efficient their number is limited to a fraction β of the initial population

$$N_{l_{c\_\max}} = \beta N_l. \tag{2}$$

The evolution of the total vector population is controlled by interaction with the state vectors generated from the system during its operation, the external codes. This dynamical evolution has mutation and stimulation features that are described next.

1) Mutation: A mutation process takes place every time an external code $\vec{y}$, coming from the system, arrives to the B-module. The mutation process begins by selecting, from the total population, a sample of p_m vectors, $\left\{\vec{x_m}\right\}$. The mutation process operates only in this part of the population and in those codes that are close to the external signal $\vec{y}$.

The mutation process depends on the affinity between the vectors $\vec{x_m}$ in the sample and the external code $\vec{y}$. When the vector $\vec{x_m}$ and the code $\vec{y}$ are far way, as in zone A of Fig. 2, no affinity is considered to exist and the code $\vec{x_m}$ is not changed. Also, in zone B there is no modification. For codes $\vec{x_C}$ in zone C, the mutation process occurs in a deterministic way. The external code $\vec{y}$ is assumed to have mass one and the vectors in zone C mass m_l. The new code in the population corresponds to the center of mass of the two entities, given by

$$\vec{x_C}(t+1) = \frac{m_l \vec{x_C}(t) + \vec{y}}{1 + m_l}. \tag{3}$$

In zone D, the mutation process works in a random way. The new position of the population vector $\vec{x_D}$ is found using a random uniform distribution for each point of the line defined by the old position of the vector and the position of the external code

$$\vec{x_D}(t+1) = \vec{x_D}(t) + \eta\left(\vec{y} - \vec{x_D}(t)\right). \tag{4}$$

When the external code appears repeatedly in the same region, the mutation process leads to a population cluster in that region, as shown in Fig. 5(b). The speed of cluster formation depends on the parameters m_l and η. The cluster code is computed by a hierarchical binary tree routine, a cluster being identified when a threshold parameter in the clustering algorithm is reached. The cluster center defines an *alert code* that is passed to the T-module to be processed as described in Section III-A. If the alert code is identified as a self code, it is eliminated from the population. Otherwise, it reports an anomaly and creates a new or improved detector in the T-module.

The mutation process is illustrated in Fig. 3 which corresponds to an external code $\vec{y} = (0.1, 0.7)$ being detected many times. A cluster is created around the external code.

It is also clear that, when either the nature of the self codes is not known or it is difficult to specify a priori, the B-module, used with a system in normal operating conditions, may be used to generate the self codes by the mutation process.

2) Stimulation: As new external codes arrive in the B-module, the mutation process destroys the initial uniformity of the vector population, resulting sometimes in a highly sparse distribution. In this case, if an atypical external code appears, its detection may become difficult. This situation is even more critical when the external code is located near the boundary of the state space or near an already formed cluster. In these cases, the mutation process has a high probability to fail because the areas C and D (Fig. 2) are depleted. To overcome this drawback, a *stimulation* or *cloning* mechanism has been included in the algorithm to create new vectors in the region where the external code appears.

The cloning mechanism is activated when the rate of external codes arriving in a neighborhood exceeds a prespecified threshold α. If the rate is below this threshold, there is no cloning and only the mutation process takes place. The number of clone vectors in the total population is limited to a maximum $N_{l_{c\_\max}}$. As long as the stimulation threshold is exceeded in a given region, clones are added to the population in locations chosen at random in the regions B to D. If the number of clone vectors has reached its maximum value and more external codes continue arriving, at a rate above the stimulation threshold, the oldest clones in the population are progressively replaced by the new external codes. After each cloning, the mutation mechanism is activated as before for a possible cluster formation.

A death mechanism is also introduced for the clone vectors. At each time, one vector from the total population is chosen at random. If it belongs to the initial N_l population nothing happens. However, if it belongs to the set of N_{l_c} clone vectors, it is eliminated with probability

$$P_{\text{die}} = \frac{N_{l_c}}{N_{l_c} + N_l}. \tag{5}$$

The stimulation mechanism is illustrated in Figs. 4 and 5. The initial population in Fig. 5(a) was exposed from time $t = 0$ to $t = 150$ to the external code $a = (0.4, 0.4)$, from $t = 151$ to $t = 200$ to the code $b = (0.7, 0.7)$ and from $t = 201$ to $t = 300$ to the code $c = (0.32, 0.32)$. Fig. 4 shows the evolution of the total number of clone vectors with an initial vector population of 200 vectors. Notice in this figure that clones only start to be created after a certain number of occurrences of the external code a. The clone population increases. After the change of external code a to b, only the random death mechanism is observed during a time interval. Following, the clones' number start increasing again until the new external code c appears. After the death mechanism, the clone population increases again until a certain saturation level. In this example the saturation level N_{l_c} has been set at 400. Fig. 5(b)–(d) shows three successive snapshots of the total population evolution with the clones denoted by a diamond symbol.

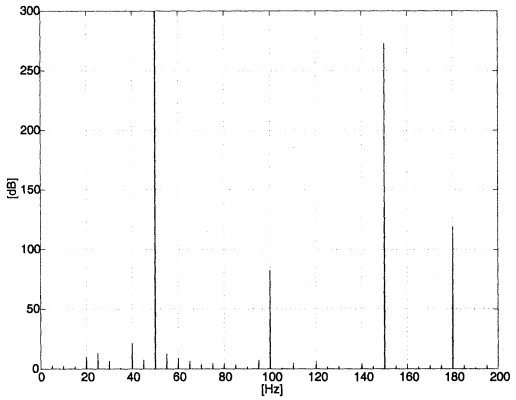

(a)

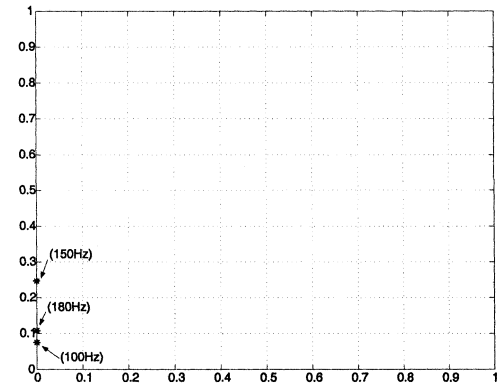

(b)

Fig. 6. (a) Normal operation frequency spectrum. The 50-Hz intensity is 16 667 dB. (b) Three self patterns at 100, 150, and 180 Hz.

Memory is a hallmark of the immune system. As in the immune system, memory features are present in the algorithm at two levels. In the T-module, the tuning of the position and range of the detectors acts as a long time memory of past anomaly situations. For the B-module, the distribution of the population, both initial population and clones, has memory features at two different time scales.

C. D-Modules

For large distributed systems like, for example, an electrical power distribution network it is not economic, in terms of computational power and communications, to keep a permanent monitoring of the whole system by a centralized facility. Therefore, in these cases it is reasonable to distribute throughout the network a large number of simple monitoring systems, which report to a central unit only when some unusual condition appears as a candidate anomaly. Depending on the nature of the transferred data to the central unit, this one may then subject this particular network node to a finer analysis.

The D-modules behave, therefore, as *anomaly-presenting* systems and may be constructed as simplified T-modules with a reduced state space. For example, to monitor the power transformers in a network, the D-modules may only process the data related to the concentration of a particular gas type or the temperature at a few critical points. In case of a potentially anomalous situation, the central unit may then require the transfer of data from other monitoring devices.

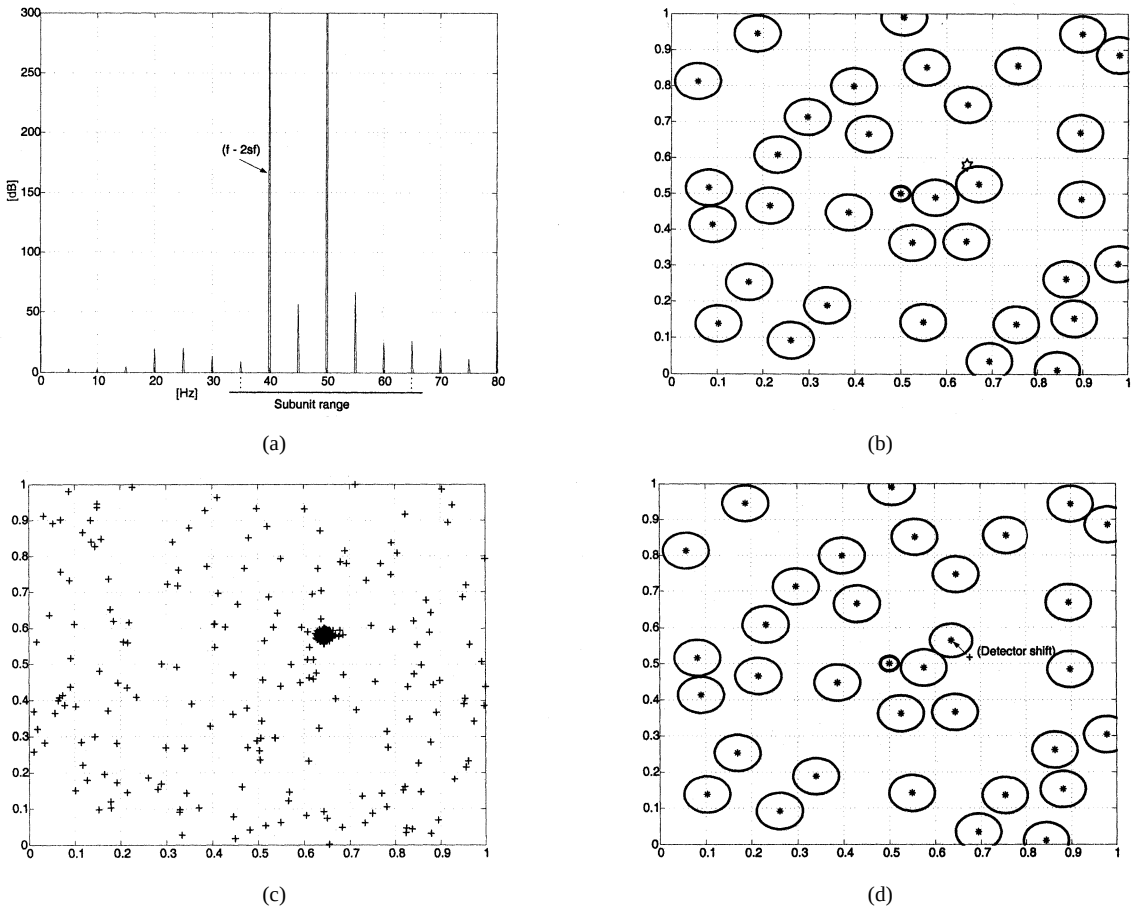

Fig. 7. Motor with one broken rotor bar. (a) Sideband frequencies and range of the subunit around 50 Hz. 50-Hz intensity = 16 667 dB, 40-Hz intensity = 425 dB. (b) Initial detectors, self pattern, and the external code. (c) Vector population after the stimulation and mutation processes. (d) Detector shift.

Although simplified, the D-modules may also be evolving units, learning both from their experience of local conditions and from periodic updates to benefit from experience collected at other points of the network.

IV. Anomaly Detection in Squirrel-Cage Motors

Squirrel-cage motors are critical components of many pieces of industrial equipment. They are fairly reliable machines, nevertheless, they do suffer degradation and occasional failure. Environment, duty cycles, and installation conditions may combine to accelerate motor failure. Their malfunction introduces costs in the industrial processes where they are inserted, these costs being often much higher than the actual cost of the motor.

These motors often experience several faults. The first group is composed by situations as overload, single phasing, locked rotor, ground fault, overvoltage, and undervoltage [15]. To monitor these faults, a simple solution consists in use protective relays to disconnect the motors in case of a faulty situation. The second group of faults can be divided into stator and rotor classes of failures, which can be primarily detected in their incipient phases: stator failures group bearings [16] and interturn faults [17], and rotor failures group broken bars [10], [11], [14] and eccentricity. The third group of faults is concerned not only with the electrical machine itself but with its interaction with the power converter [18] and mechanical load. Fault situations as an unbalanced power supply and time-varying loads [19] are included in this group.

It is important to emphasize that the algorithm proposed is not appropriate to any fault type. The method presents specific characteristics that make it more efficient to a restrict but high frequent-fault situations for the squirrel-cage motor.

- When the failure is gradual, for example, broken rotor bars, the algorithm using its mutation and cloning processes is capable to gradually trace the fault appearance, thus allowing early fault detection and potentially a predictive maintenance [20];
- For situations where the machine is inserted in a production unit, it is normally difficult to distinguish a normal operation of the motor from a potential failure one using only the stator current frequency spectrum as the fault indicator. The algorithm through its capability to distinguish the self (normal operation condition) from a nonself (faulty operation) state of the machine, allows a solution to this problem as shown next.

It was based on these assumptions that we have selected three typical fault situations to be studied. One was the broken rotor bars fault. The second fault situation has the machine operating with an oscillatory load (characterizing a certain normal machine operation) and the case of an unbalanced power supply. The third fault situation considers again an oscillatory load but now with a broken rotor bar occurring in the motor.

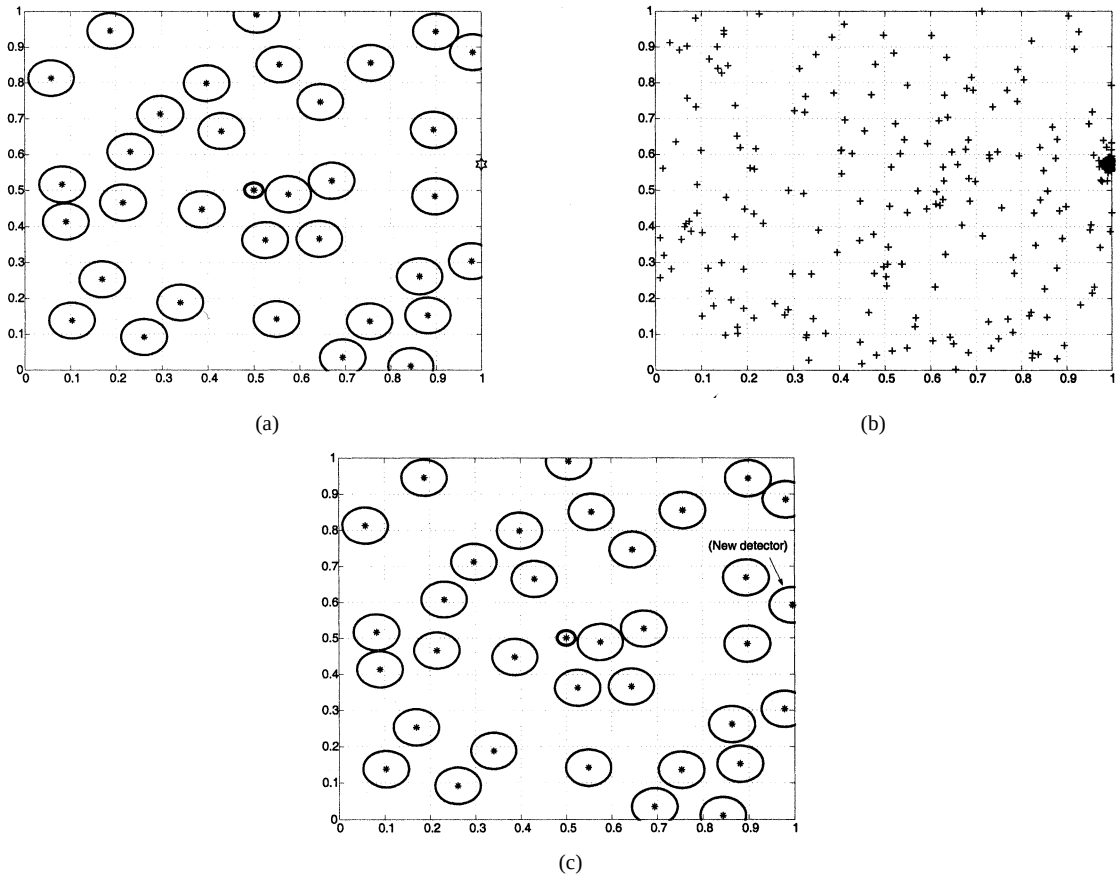

Fig. 8. Motor with four broken rotor bars. (a) Initial detectors, self pattern and the external code. (b) Vector population after the stimulation and the mutation processes. (c) A new detector is created.

A variety of fault detection techniques have been proposed [8]–[14] for the squirrel-cage motor. Each one addresses a specific failure in one of the three motor components: the stator, the rotor, or the bearings. The signals to be monitored may be stator voltages and currents, output torque, rotor position and speed, air-gap flux density, temperature, and vibrations. A large amount of research has concerned the use of stator current spectrum for fault detection, including fault classification [21]–[24]. The presence of some frequency components has been shown to be the signature of a fault condition.

Most methodologies based on the stator current spectrum are based on the assumption that the current drawn by a normal motor has only a significantly large component at the supply frequency. A machine malfunction would manifest itself by the appearance of other significant components, some frequencies being related to specific faults. However, it is difficult to distinguish in this way a normal operating condition from a potential failure. This is because spectral components may arise from a number of sources, including those related to normal operating conditions. Harmonic components may exist, caused by the motor design, by the power network or by fluctuations in the load torque, which are not related with an abnormal motor condition.

To consider a single component spectra as the representative pattern of normal motor condition is not correct. It is the actual current spectra, obtained when the motor is inserted in the production unit in typical conditions, that characterizes the *normal operating conditions*. It is this frequency spectrum, with or without harmonics, that characterizes the *self* state of the machine.

Instead of analyzing all spectrum as the majority of the current algorithms do, our algorithm uses a set of D-modules localized at specific frequency intervals in the stator current spectrum where most frequent faults occur. Using the patterns that characterize the normal motor operation to build the self, the method is capable of building a series of fault detectors $\vec{x}$ that, when an anomaly pattern occurs inside one of them, an anomaly of type x can be reported. Notice that to avoid overreaction to spurious situations, each detector is equipped with a counter and reports an anomaly only if the offending vector occurs more than a predefined number of times. Thus, there is no diversity of meaning since it has the capability to classify the most frequent anomalies.

A. Fault Detection: Results and Discussion

The stator current is sampled and converted to the frequency domain using a discrete Fourier transform, thus accounting for a steady-state operation of the electrical machine. A sequence of spectra is obtained by a moving window on the current data. Only those harmonics with amplitude greater than 50 dB and frequencies below 200 Hz are kept. The 200-Hz upper limit was chosen because most frequencies related to squirrel-cage motor faults occur in this interval. Harmonic amplitudes are normalized by the amplitude of the supply frequency.

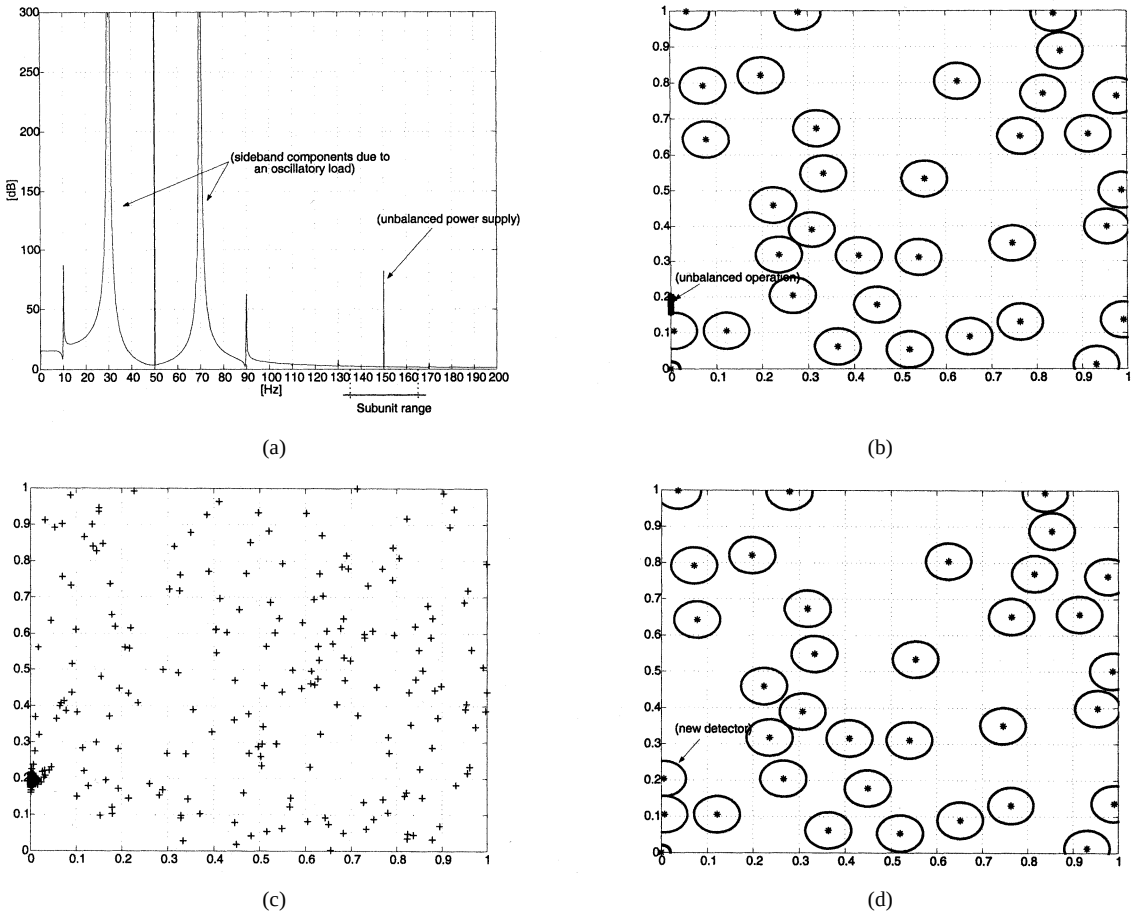

Fig. 9. Motor with oscillatory load and unbalanced power supply. (a) Sideband frequency components and range of the subunit around 150 Hz. Intensities: (30 Hz) = 8740 dB; (50 Hz) = 16 667 dB; (70 Hz) = 5503 dB. (b) Initial detectors, self pattern, and external codes. (c) Vector population after the stimulation and mutation processes. (d) New detector created to monitor unbalanced operation.

A detailed anomaly detection system must consider the overall frequency spectrum pattern. Even discretizing the spectrum, this implies monitoring a very high-dimensional space, a process that requires considerable computer power. On the other hand, it is not necessary to be monitoring all frequencies in full detail all the time. The solution is to segment our anomaly-detection system into several subunits, each one covering a frequency interval in the spectrum. The frequency resolution of all the subunits need not be same because, from experience, we already know what frequency intervals need to be monitored in more detail. All the subunits work in a similar fashion, the overall operating mode of the system being such that at each time only one subunit is active but the active one changes periodically. In this way, an adequate fine covering of the energy spectrum is implemented, while keeping the computation requirements at a reasonable level.

A segmentation scheme of this type is applicable to any system where a good resolution of the operation conditions is desired. However, if, at the same time, an overall continuous monitoring of the whole system is necessary, the outputs of the subunits may be looked at as components of a global coding vector that is sent for analysis to a central system. The central system may then operate on a slower time schedule.

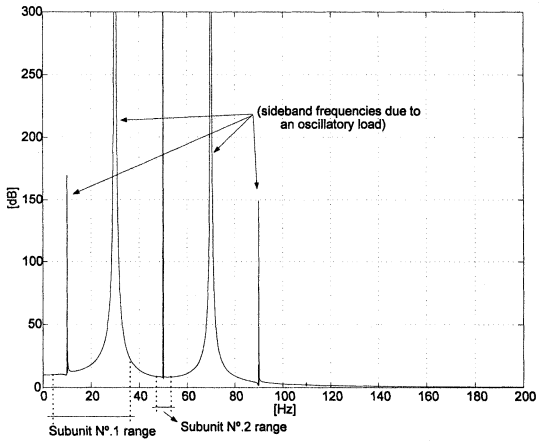

Fig. 10. Motor with oscillatory load and broken rotor bars. Sideband frequency components due to the load and range of subunits $N^o.1$ and $N^o.2$ around 50 and 20 Hz.

1) Results: The operation of the subunits is now illustrated using laboratory results from normal conditions and from three typical fault situations.

Each subunit monitors a frequency interval around a frequency value f_D. The frequency interval is divided in two equal parts. For each part, the integral of the corresponding

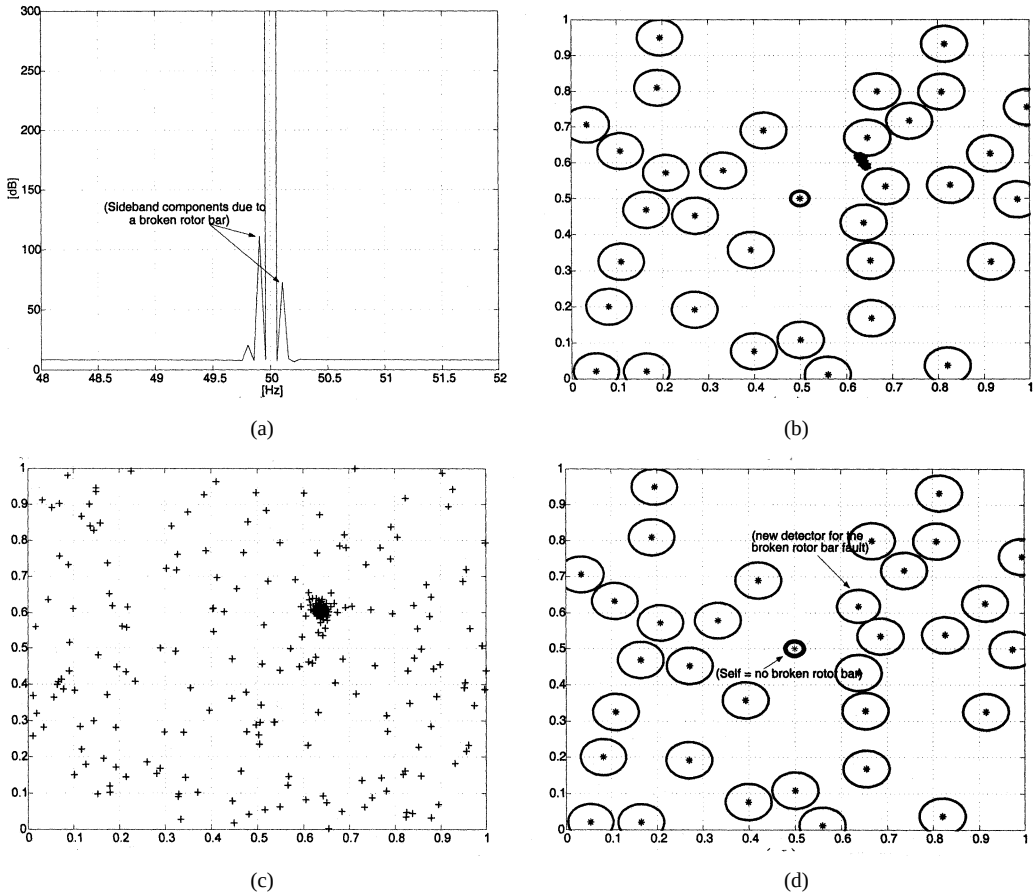

Fig. 11. Motor with oscillatory load and broken rotor bar. (a) Sideband frequency components and range of the subunit $N^o.1$ around 50 Hz. (b) Initial detectors, self pattern, and external codes. (c) Vector population after the stimulation and mutation processes. (d) New detector code created to monitor the faulty situation.

spectrum is computed, obtaining a data pair that is sent as the external code to the algorithm. The lower and higher intervals correspond to the abscissa and ordinate coordinates in the figures.

As shown in Fig. 6(a), even in normal operation, the stator current spectrum can display, in addition to the 50-Hz component, other significant frequency components (near 100, 150, and 180 Hz). Asymmetry in the power supply and misalignment are at the origin of these frequency components. Possible subunits covering these frequencies detect these components as the *self* patterns of the motor, characterizing its normal condition state. Fig. 6(b) shows the *self* patterns of three of these subunits. Notice that when the subunits are centered exactly at 100, 150, and 180 Hz, the slip frequency makes the harmonics to contribute only to the integrated spectrum of the higher interval. We now illustrate the three fault situations, namely the case of rotor broken bars, the case of oscillatory load and unbalanced power supply, and the case of oscillatory load and rotor broken bars.

Case 1: Broken Rotor Bars: Broken rotor bars generate spectrum lines at frequencies

$$f_1 = f \pm (2ks)f \tag{6}$$

with s being the slip frequency, f the supply frequency, and k an integer value (1, 2, 3,...). The amplitude of the sideband frequencies measures the seriousness of the anomaly.

A subunit centered at the supply frequency (50 Hz), as shown in Fig. 7(a), has been tested using laboratory measurements of the stator current of a squirrel-cage motor with different numbers of broken bars.

For the case of one broken bar, Fig. 7(a) shows the current spectrum. The initial population of T-detectors $(n = 33)$ and the self pattern of this subunit are shown in Fig. 7(b). As external codes come from the system [the hexagonal symbol in Fig. 7(b)], the B-module, through the stimulation and mutation processes, creates a new distribution of the vector population [Fig. 7(c)]. The interaction between the B-module and the T-module leads to the detector shift shown in Fig. 7(d) and to the reporting of a motor anomaly.

A more severe situation is shown in Fig. 8(a) when the motor has four broken bars. The subunit now is the same as before, centered at 50 Hz. With four broken bars, the amplitude of the sideband components has increased, creating external codes near the boundary of state space [Fig. 8(a)]. After the stimulation and mutation processes illustrated in Fig. 8(b), a new detector is created [Fig. 8(c)] to monitor and report this anomaly.

Case 2: Oscillatory Load Plus an Unbalanced Power Supply: Fault detection schemes for squirrel-cage motors generally assume that the load torque is constant. If the load torque varies with the rotational speed, then the motor current spectral harmonics produced by the load can overlap the harmonics caused by the fault conditions. The interaction of the effects on the actual stator current spectrum caused by the fault condition of an unbalanced power supply and the torque oscillations is studied in this case.

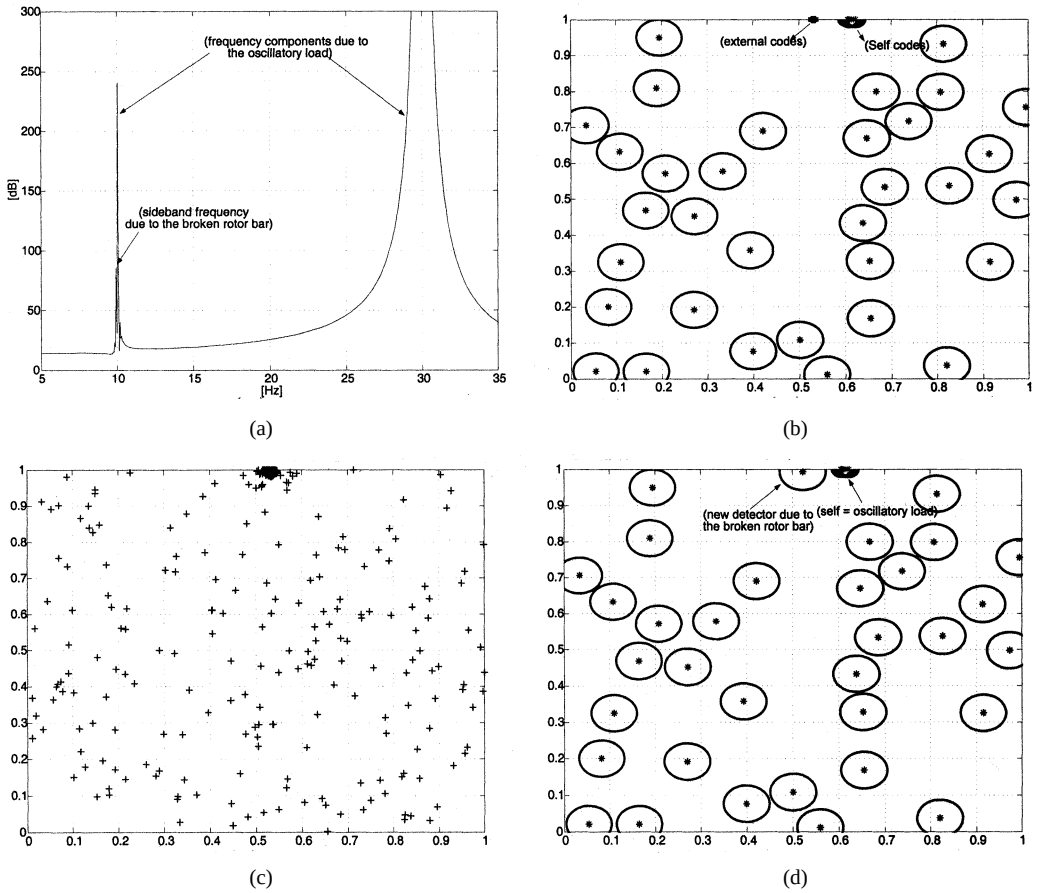

Fig. 12. Motor with oscillatory load and broken rotor bar. (a) Sideband frequency components and range of the subunit $N^o.2$ around 20 Hz. (b) Initial detectors, self pattern, and external codes. (c) Vector population after the stimulation and mutation processes. (d) New detector created to monitor the faulty situation.

An oscillation in the load torque at a multiple m of the rotor speed creates spectral lines at frequencies

$$f_{\text{load}} = f(1 \pm km(1-s)) \tag{7}$$

where $k = 1, 2, 3, \ldots$. Sideband frequency components of this type are shown in Fig. 9(a).

With an unbalanced power supply, a negative-sequence voltage appears at the stator winding. This creates harmonics at frequency components

$$f_{umb} = f(1 \pm k(1-s)). \tag{8}$$

The power supply frequency remains at 50 Hz. Therefore, a subunit centered at 150 Hz detects faults of these types. Already, when operating in normal conditions there is an harmonic of small amplitude near this frequency which will characterize the self configuration of the motor. When a situation of unbalanced operation arises, the magnitude of this harmonic increases, generating new external codes, as shown in Fig. 9(b). The external codes for the unbalanced condition interact with the B-module resulting in the final vector population shown in Fig. 9(c). This then originates a new detector in the T-module of this subunit [Fig. 9(d)] and an anomaly is reported.

Case 3: Oscillatory Load Plus Broken Rotor Bar: Oscillatory motor loads generate forces that impact the dynamic performance of any squirrel-cage motor. Related mechanical stresses in the rotor mainly contribute to a failure of broken rotor bars. Fig. 10 shows the stator current spectrum obtained for this situation. The highest frequency components due to the oscillatory load are indicated in the figure at 10, 30, 70, and 90 Hz.

A set of subunits with different ranges could be distributed by the spectrum. We show in Fig. 10 two subunits designed to detect a fault condition in this case. Subunit $N^o.1$ was centered at 50 Hz with a range of ± 2 Hz, while subunit $N^o.2$ was centered at 20 Hz with a range of ± 15 Hz. Notice that while subunit $N^o.2$ covers the supply frequency to detect any anomaly, subunit $N^o.1$ covers a possible frequency interval containing harmonics due to the oscillatory load.

Subunit $N^o.1$ centered at the supply frequency (50 Hz) is shown in Fig. 11(a). The sideband frequencies due to a broken rotor bar are indicated in the spectrum. The initial population of T-detectors and the self pattern of this subunit (self-oscillatory load but no broken bar) are shown in Fig. 11(a). As external codes come to the subunit (the dark symbols in Fig. 11(b)), the B-module, through the stimulation and mutation processes, creates a new distribution of the vector population [Fig. 11(c)]. The interaction between the B-module and the T-module leads to a shift of the detector nearest the external codes. Fig. 11(d) shows the new detector code, which now has an increased affinity to this type of anomaly.

Fig. 12(a) shows subunit $N^o.2$ centered at frequency 20 Hz. The harmonics due to the oscillatory load and the broken rotor bar are indicated in the spectrum. Self codes indicated in Fig. 12(b) correspond to a case without any fault, only due to

the oscillatory load. When a broken bar arises, a new harmonic appears in the spectrum [Fig. 12(a)], generating new external codes, as shown in Fig. 12(b). The external codes interact with the B-module resulting in the final vector population shown in Fig. 12(c). A new detector is generated in the T-module of this subunit [Fig. 11(d)] and the anomaly is reported.

V. Conclusions

1) Equipments of the same type and equal ratings have different aging processes, depending on their particular location in the industrial process and stress conditions. Therefore, normal operating conditions of the same type of equipment vary over a wide range of possibilities. On the other hand, it is virtually impossible to make a complete catalog of all the possible and probable anomaly situations. By adapting itself to the actual operating conditions of the system, fault detection based on the specific immunity response algorithms seems to be an adequate device to characterize the particular nature of the normal conditions as well as to react to new and unexpected anomaly situations.
2) By being able to detect anomaly conditions at an early developing stage, immunity-based systems may provide substantial cost savings in industrial processes and be an useful tool to develop preventive maintenance schedules.
3) In the T- plus B-module system developed in this paper, each detected anomaly corresponds to a well defined code in the detection system. The code of the detected anomaly is then a useful piece of information for diagnosis and corrective measures.
4) By trial and chance over millions of years, nature's evolutionary processes have found very efficient processes to deal with all kinds of hostile environments. To obtain inspiration from these natural mechanisms seems to be a sensible approach. However, some of the features of the biological processes are domain specific and depend on the cell hardware that is used. Therefore, it is appropriate to obtain algorithmic inspiration from nature, but it would be ill advised to copy all the details of the biological process.
5) Organisms, as a first barrier to infection, also protect themselves by nonspecific mechanisms like macrophages, cell apoptosis, etc. These nonspecific mechanisms have a parallel with the devices used in the past for the protection of electrical power systems (circuit breakers, partial network shutdowns, etc.). What this analogy suggests is that it is high time to move beyond the nonspecific protection mechanisms toward specific anomaly detection devices. Nature has been doing it for millions of years.

Acknowledgment

The authors are grateful to A. J. M. Cardoso from the University of Coimbra for providing the motor fault experimental data.

References

[1] P. C. Doherty and J. P. Christensen, "Accessing complexity: The dynamics of virus-specific T cell responses," *Annu. Rev. Immunol.*, vol. 18, pp. 561–592, 2000.
[2] A. A. Freitas and B. Rocha, "Population biology of lymphocites: The flight for survival," *Annu. Rev. Immunol.*, vol. 18, pp. 83–111, 2000.
[3] R. W. Dutton, L. M. Bradley, and S. L. Swain, "T cell memory," *Annu. Rev. Immunol.*, vol. 16, pp. 201–223, 1998.
[4] J. Banchereau, F. Briere, C. Caux, J. Davoust, S. Lebecque, Y.-J. Liu, B. Pulendran, and K. Palucka, "Immunobiology of dendritic cells," *Annu. Rev. Immunol.*, vol. 18, pp. 767–811, 2000.
[5] R. M. Zinkernagel, "On immunological memory," *Philos. Trans. R. Soc. London*, vol. 355, pp. 369–371, 2000.
[6] D. Dasgupta and S. Forrest, "Novelty detection in time series data using ideas from immunology," presented at the 5th Int. Conf. Intelligent Systems, Reno, NV, June 19–21, 1996.
[7] J. Timmis, M. Neal, and J. Hunt, "An artificial immune system for data analysis," *Biosystems*, vol. 55, pp. 143–150, 2000.
[8] J. Penman, M. N. Dey, A. J. Tait, and W. E. Bryan, "Condition monitoring of electrical drives," *Proc. Inst. Elect. Eng.*, pt. B, vol. 133, no. 3, pp. 142–148, 1986.
[9] P. Goode and M.-Y. Chow, "Using a neural/fuzzy system to extract knowledge of incipient fault in induction motors," *IEEE Trans. Ind. Electron.*, vol. 42, pp. 131–138, Apr. 1995.
[10] K. R. Cho, J. H. Lang, and S. D. Umans, "Detection of broken rotor bars in induction motors using state and parameter estimation," *IEEE Trans. Ind. Applicat.*, vol. 28, pp. 702–709, May/June 1992.
[11] R. F. Walliser and C. F. Landy, "Determination of interbar current effects in the detection of broken rotor bars in squirrel cage induction motors," *IEEE Trans. Energy Conversion*, vol. 9, pp. 152–158, Mar. 1994.
[12] P. J. McCully and C. F. Landy, "Evaluation of current and vibration signals for squirrel cage induction motor condition monitoring," in *Proc. Eight Int. Conf. Electrical Machines and Drives*, 1997, pp. 331–335.
[13] F. Filippetti, G. Franceschini, C. Tassoni, and P. Vas, "AI techniques in induction machine diagnosis including the speed ripple effect," *IEEE Trans. Ind. Applicat.*, vol. 34, pp. 98–108, Jan./Feb. 1998.
[14] J. Milimonfared, H. M. Kelk, S. Nandi, A. D. Minassians, and H. A. Toliyat, "A novel approach for broken-bar detection in cage induction motors," *IEEE Trans. Ind. Applicat.*, vol. 35, pp. 1000–1006, Sept./Oct. 1999.
[15] A. H. Bonnett and G. C. Soukup, "Cause and analysis of stator and rotor failures in three-phase squirrel-cage induction motors," *IEEE Trans. Ind. Applicat.*, vol. 28, pp. 921–937, July/Aug. 1992.
[16] H. A. Toliyat and T. A. Lipo, "Transient analysis of cage induction machines under stator, rotor bar and end ring faults," *IEEE Trans. Energy Conversion*, vol. 10, pp. 241–247, June 1995.
[17] A. J. M. Cardoso, S. M. A. Cruz, and D. S. B. Fonseca, "Inter-turn stator winding fault diagnosis in three-phase induction motors by Park's vector approach," *IEEE Trans. Energy Conversion*, vol. 14, pp. 595–598, Sept. 1999.
[18] D. Kastha and A. K. Majumdar, "An improved starting strategy for voltage-source inverter fed three phase induction motor drives under inverter fault conditions," *IEEE Trans. Power Electron.*, vol. 15, pp. 726–732, July 2000.
[19] R. R. Schoen and T. G. Habetler, "Effects of time-varying loads on rotor fault detection in induction machines," *IEEE Trans. Ind. Applicat.*, vol. 31, pp. 900–906, July/Aug. 1995.
[20] M. M. O'Kane and M. J. Sander, "Intelligent motors move to the forefront of predictive maintenance," *IEEE Ind. Applicat. Mag.*, vol. 6, pp. 47–51, Sept./Oct. 2000.
[21] M. E. H. Benbouzid, M. Vieira, and C. Theys, "Induction motors' faults detection and localization using stator current advanced signal processing techniques," *IEEE Trans. Power Electron.*, vol. 14, pp. 14–22, Jan. 1999.
[22] B. Yazici and G. B. Kliman, "An adaptive statistical time-frequency method for detection of broken bars and bearing faults in motors using stator current," *IEEE Trans. Ind. Applicat.*, vol. 35, pp. 442–452, Mar./Apr. 1999.
[23] R. R. Schoen, B. K. Lin, T. G. Habetler, and S. Farag, "An unsupervised on-line system for induction motor fault detection using stator current monitoring," *IEEE Trans. Ind. Applicat.*, vol. 31, pp. 1280–1286, Nov./Dec. 1995.
[24] R. Natarajan, "Failure identification of induction motors by sensing unbalanced stator currents," *IEEE Trans. Energy Conversion*, vol. 4, pp. 585–590, Dec. 1989.

P. J. Costa Branco (M'92) is currently an Assistant Professor in the Department of Electrical and Computing Engineering, Section of Electrical Machines and Power Electronics, Instituto Superior Técnico (IST), Lisbon, Portugal, and has been with the Mechatronics Laboratory of IST since 1992. His research areas are in control of electrical drives, systems modeling, and control using soft-computing techniques, and he is presently engaged in research on modeling and control techniques for piezoelectric actuators. He is the author of papers that have appeared in international scientific journals such as the IEEE TRANSACTIONS ON MAGNETICS, IEEE TRANSACTIONS ON SYSTEMS, MAN, AND CYBERNETICS, IEEE TRANSACTIONS ON FUZZY SYSTEMS, IEEE TRANSACTIONS ON INDUSTRIAL ELECTRONICS, IEEE TRANSACTIONS ON AEROSPACE AND ELECTRONIC SYSTEMS, *Pattern Recognition Letters, Fuzzy Sets and Systems, and European Transactions on Electrical Power Engineering.* He has been a referee for international scientific journals and participated on the boards of international meetings.

J. A. Dente graduated in electrical engineering and received the Ph.D. degree in electrical engineering from the Instituto Superior Técnico (IST), Lisbon, Portugal, in 1975 and 1986, respectively.

From 1989 to 1993, he was an Associate Professor at IST, where he is currently a Full Professor in the area of electrical machines in the Department of Electrical and Computing Engineering, Section of Electrical Machines and Power Electronics. He is also with the Mechatronics Laboratory, IST, where he has been the Scientific Coordinator since 1993. He has authored more than 30 scientific articles published in refereed journals and books, and more than 40 articles in refereed conference proceedings. His primary areas of interest are in electrical machines, motion control, and he presently is engaged in research on advanced learning control techniques for electromechanical systems.

R. Vilela Mendes graduated in electrical engineering from the Instituto Superior Técnico (IST), Lisbon, Portugal, in 1960, and received the Ph.D. degree in physics from the University of Texas at Austin in 1970.

He is a Senior Researcher at IST and a collaborator in its Mechatronics Laboratory. He has authored more than 100 papers published in international journals on topics including physics, nonlinear dynamics, signal processing, and computer science. His main interests are currently nonlinear dynamics of multi-agent systems and quantum information.